Available online at www.sciencedirect.com

ScienceDirect

IFAC Papers Online CONFERENCE PAPER ARCHIVE

IFAC PapersOnLine 53-1 (2020) 410–415

Yaw Angle Control of Heavy Commercial Road Vehicle with Faulty Brake ⋆

Radhika Raveendran * **Devika K. B.** ** **Harshal Patil** *** **Shankar C. Subramanian** ****

* *Ph.D. Scholar, Department of Engineering Design, IIT Madras, Chennai, India. (e-mail: radhikaraveendran@gmail.com)*
** *Post Doctoral Fellow, Department of Engineering Design, IIT Madras, Chennai, India. (e-mail: devikakb@gmail.com)*
*** *M. S. Scholar, Department of Engineering Design, IIT Madras, Chennai, India. (e-mail: harshalp1092@gmail.com)*
**** *Professor, Department of Engineering Design, Indian Institute of Technology Madras, Chennai 600 036, India. (e-mail: shankarram@iitm.ac.in)*

Abstract: Faults in an air brake system affect the performance of Heavy Commercial Road Vehicles (HCRVs). One of the major faults in the air brake system is the "out-of-adjustment"of pushrod due to excessive brake wear, which may cause a significant yaw angle deviation from the current path and an increase in stopping distance. Hence, this paper aims to design a controller that would maintain the vehicle's directional stability under brake fault scenario. In order to design such a controller, knowledge of vehicle side slip angle is essential, but this is not a measurable quantity. Hence, an Artificial Neural Network (ANN) based estimation scheme for side slip angle prediction is also proposed. As an output regulator problem, Sliding Mode Control (SMC) was used for correction of yaw angle under brake fault scenario through appropriate steering angle input. This controller provided a percentage correction of yaw angle of 93.4 % and 99.8 % respectively for fully laden and fully unladen vehicle on a high friction tire road interface surface, and the same corresponding to a low friction tire road interface was 99.8 % and 98.9 % respectively.

Keywords: Sliding Mode controller (SMC), yaw angle correction, Artificial Neural Network (ANN), side slip angle, Heavy Commercial Road Vehicle (HCRV)

1. INTRODUCTION

Faults in the air brake system can affect yaw stability and stopping distance in Heavy Commercial Road Vehicles (HCRVs). Major faults in the air brake system are out of adjustment of pushrod (a critical component in the air brake system) and leaks in the system. Radlinski et al. (1982) found that a drop in brake torque occurs due to increase in pushrod stroke. The variation of brake torque with respect to pushrod adjustment is shown in Fig. 1 (Dunn et al. (2012)). When the stroke length is beyond a specified limit (for example, 44.45 mm (1.75 inch) for a type 20 brake), the brake torque reduces drastically. Various model based pushrod stroke length prediction schemes have been developed by Kandt et al. (2001), Subramanian et al. (2006), Dhar (2010) and Ramarathnam et al. (2011). These methods are limited to specific set of operating conditions and were not evaluated for various road and vehicle load conditions. Raveendran et al. (2018) developed an ANN based prediction scheme to predict the pushrod stroke from the knowledge of brake chamber pressure and evaluated for different road and vehicle load conditions. The author also addressed the influence of pushrod stroke variation beyond its readjustment limit on vehicle braking performance.

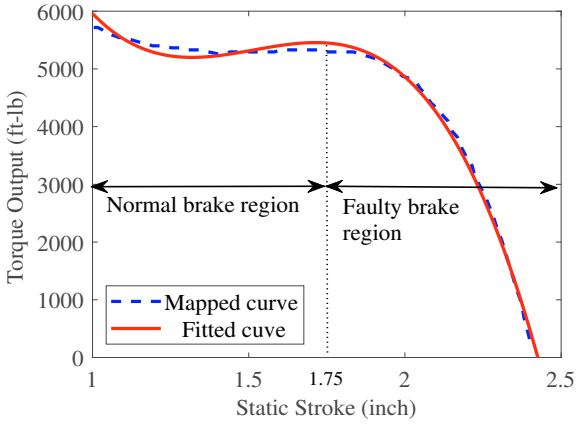

Fig. 1. Variation of brake torque with pushrod stroke for a type 20 brake chamber (Dunn et al. (2012))

Braking with a faulty brake during a straight line maneuver may result in a deviation of vehicle from its specified

⋆ Research supported by the Ministry of Skill Development and Entrepreneurship), Government of India, through the grant EDD/14-15/023/MOLE/NILE.

10.1016/j.ifacol.2020.06.069

path, which can be viewed as a significant yaw angle deviation. If an improper steering command is then provided by the driver, the vehicle may become unstable resulting in accidents. Therefore, a robust control system is essential to assist the driver to keep the vehicle stable on the desired path especially under brake fault situations. In this context, the main objective of this paper is to design a controller to maintain the yaw angle to a desired value under brake fault scenario by giving a controlled steering angle command. Here, the proposed methodology works in such a way that, whenever a brake fault is detected, the controller gets activated and provides the necessary yaw angle correction.

The present study uses a combined braking and steering vehicle model, which is a nonlinear one. Hence, it was decided to design a nonlinear control strategy for the problem at hand. Also, possible occurrences of parametric uncertainties and external disturbance during on-road vehicle operation demands the need for a robust control technique. Over the last two decades, various studies have been carried out on yaw stability controller design. Sliding mode control (SMC), being suitable for nonlinear systems as well as being a robust control strategy, has been successfully applied to numerous applications due to its inherent performance robustness in the presence of modelling uncertainties and external disturbances (Hebden et al. (2003); Kazemi and Janbakhsh (2010); Zhou and Liu (2010)). SMC provides this robustness in two ways. Initially, a sliding surface is selected, which provides an appropriate sliding motion. Later on, a control equations is designed, which ensures the system to reach and then remain on the sliding surface. By considering its robustness property to external disturbances and parameter uncertainties, this paper also uses the same for yaw angle controller design. Since the vehicle side slip angle is needed for the controller design, an Artificial Neural Network (ANN) based side slip angle estimation scheme is also presented in this paper.

The organization of this paper is as follows. Section 2 presents the vehicle model. An estimation scheme for side slip angle using ANN is given in Section 3. Controller design based on SMC and the simulation results are explained in the Section 4 and Section 5 respectively. Section 6 concludes the paper.

2. THE VEHICLE MODEL

The two track model shown in Fig. 2 was selected for the current study. The degrees of freedom (3 DOF) associated with this model are the yaw rate, roll rate, and vehicle side slip angle. The lateral dynamics of the two track vehicle model (Abe (2015)) is discussed below. The equation of vehicle motion in lateral direction is

$$\begin{aligned} &mV_x(t)\dot{\beta}(t) + 2(C_{\alpha f} + C_{\alpha r})\beta(t) \\ &\quad + \left[mV_x(t) + \frac{2(C_{\alpha f}l_f - C_{\alpha r}l_r)}{V_x(t)}\right]\dot{\psi}(t) \\ &\quad - m_s h_s \ddot{\phi}_s(t) = 2C_{\alpha f}\delta(t)\,, \end{aligned} \tag{1}$$

where m and $V_x(t)$ are the mass and the longitudinal speed of vehicle respectively, $C_{\alpha f}$, $C_{\alpha r}$ are the cornering stiffness of each front tire and rear tire respectively. l_f and l_r are the distances of the front tire and the rear tire respectively from the CG of the vehicle. m_s and h_s are the sprung mass of the vehicle and the height of CG of sprung mass from the roll axis respectively. ψ(t), ϕ_s(t), $\delta(t)$, and β(t) are yaw angle, roll angle, steering angle, and the vehicle side slip angle respectively.

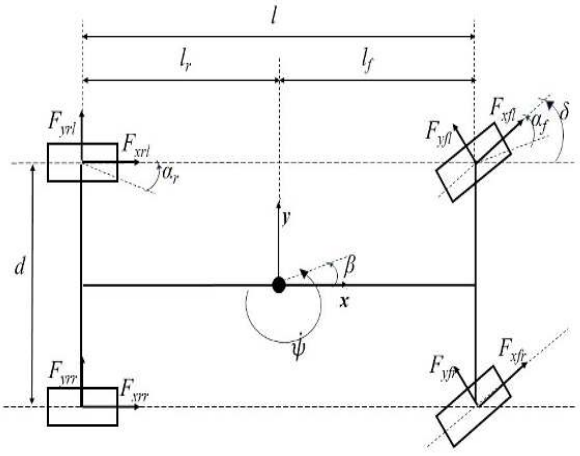

Fig. 2. Two-track model of a vehicle performing a left turn

The equation governing the yaw motion is

$$\begin{aligned} &2(C_{\alpha f}l_f + C_{\alpha r}l_r)\beta(t) + I_z\ddot{\psi}(t) \\ &\quad + \left[\frac{2(C_{\alpha f}l_f^2 + C_{\alpha r}l_r^2)}{V_x(t)}\right]\dot{\psi}(t) = 2C_{\alpha f}l_f\delta(t)\,, \end{aligned} \tag{2}$$

where, I_z is the moment of inertia about the z axis. The equation governing the roll motion is

$$\begin{aligned} &-m_s h_s V_x(t)\dot{\beta}(t) - m_s h_s V_x(t)\dot{\psi}(t) + I_x\ddot{\phi}_s(t) \\ &\quad + C_\phi\dot{\phi}_s(t) + (k_\phi - m_s g h_s)\phi_s(t) = 0\,, \end{aligned} \tag{3}$$

where, I_x is the moment of inertia about the x axis, k_ϕ and C_ϕ are the roll stiffness and roll damping respectively, g is the acceleration due to gravity.

The state space representation of (1), (2), and (3) is given by

$$\dot{\mathbf{x}}(t) = \mathbf{A}\mathbf{x}(t) + \mathbf{b}u(t), y(t) = \mathbf{c}.\mathbf{x}(t), \tag{4}$$

where, $\mathbf{A}$, $\mathbf{b}$, and $\mathbf{c}$ are state matrix, input vector, and output vector respectively. $\mathbf{x}(t)$ and $u(t)$ are the state vector and the control input and are given by

$$\mathbf{x}(t) = \left[\beta(t)\ \psi(t)\ \dot{\psi}(t)\ \phi_s(t)\ \dot{\phi}_s(t)\right]^T, \tag{5}$$

$$u(t) = \delta(t). \tag{6}$$

Here, the output is,

$$\begin{aligned} y(t) &= \begin{bmatrix}0\\1\\0\\0\\0\end{bmatrix} . \begin{bmatrix}\beta(t)\\ \psi(t)\\ \dot{\psi}(t)\\ \phi_s(t)\\ \dot{\phi}_s(t)\end{bmatrix} \\ &= \psi(t). \end{aligned} \tag{7}$$

The above nonlinear model was used to design a sliding mode controller for correcting the yaw angle deviation

during brake fault scenario. The state variables used in the current study are yaw rate, roll rate, yaw angle, roll angle, and the vehicle side slip angle. The overall block schematic of the controller is shown in Fig. 3. The fault flag activates the controller to give the steering angle command at the time of brake fault. Here, the variables required for

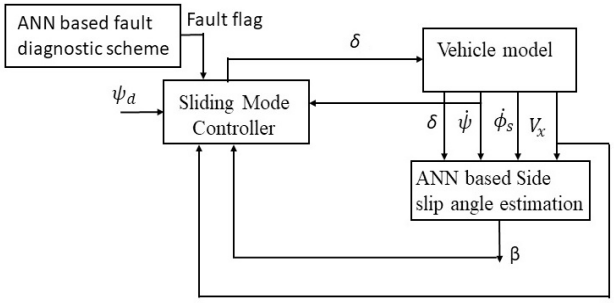

Fig. 3. Overview of yaw angle correction controller

implementing the controller are yaw rate, vehicle longitudinal speed and side slip angle. Among these, vehicle longitudinal speed and side slip angle are not readily available as measurements in practice. Many studies have focussed on the estimation of longitudinal speed using Adaptive Kalman Filter (AKF) and Unscented Kalman Filter (UKF) (Song et al. (2002); Chu et al. (2010); Gao et al. (2013)). Hence, the interest of this study is the estimation of side slip angle and its use in the design of the yaw angle controller. Consequently, it was assumed that the vehicle longitudinal speed is available for the controller design. An ANN based side slip angle estimation scheme was developed and is explained in section 3. Also, the desired yaw angle is taken as 0^o for a straight line maneuver.

3. SIDE SLIP ANGLE ESTIMATION USING ARTIFICIAL NEURAL NETWORK

An Artificial Neural Network (ANN), which is a computational model based on the structure and functions of biological neural networks, basically consists of input layers, hidden layers and output layers. The weights of hidden layers (weighted connection of nodes) have to be adjusted to get an accurate ANN model. In this study, an estimation scheme using ANN was developed to estimate the side slip angle. Figure 4 shows the basic structure of ANN model for estimating side slip angle. Based on (1), the inputs needed to develop the ANN model were identified as yaw rate, roll rate, vehicle longitudinal speed, and the vehicle steering wheel angle. The output of the model is the side slip angle. In order to train the multilayer feed-forward network, a back propagation algorithm was used.

3.1 Data Collection and the estimation scheme

The training data set needed to train the ANN model were collected with combinations of following test scenarios:

(1) Both straight line maneuver and steady state circle with radius of 100 m with an initial longitudinal speed of 22.22 m/s were considered and the brake application time was an interval of 10 s.

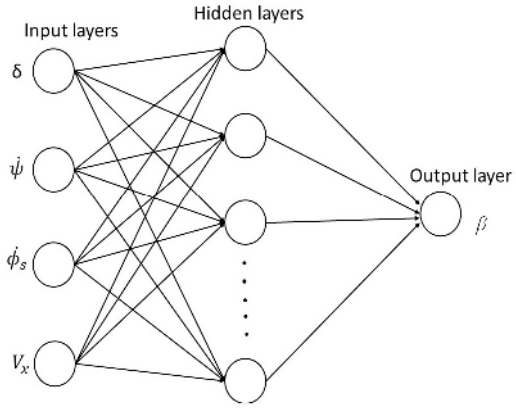

Fig. 4. ANN model for side slip angle estimation

(2) Full brake application was considered.
(3) Maximum tire road friction coefficients considered are 0.8 (dry road surface), 0.5 (wet road surface), and 0.35 (snowy road surface).
(4) Both normal and faulty brake conditions were considered. Here, the fault scenarios were 10 %, 20 % and 30 % torque reduction from the full load torque corresponding to excessive pushrod length.
(5) Fully laden and fully unladen load conditions were considered.

Table 1. Vehicle parameters.

Parameters	Value	Parameters	Value
Mass (Laden), kg	16200	Mass (Unladen), kg	4700
FAW [1] (Laden), kg	6000	FAW (Unladen), kg	2350
CG [2] Height, (Laden), m	1.3	CG Height, (Unladen), m	1
I_z (Laden), kgm^2	100000	I_z (Unladen), kgm^2	39000
I_x (Laden), kgm^2	19866.3	I_x (Unladen), kgm^2	6135.9
$C_{\alpha f}$ (Laden), N/rad	183250	$C_{\alpha f}$ (Unladen), N/rad	78803
$C_{\alpha r}$ (Laden), N/rad	226207.5	$C_{\alpha r}$ (Unladen), N/rad	53922.5
k_ϕ, Nm/rad	642902	C_ϕ, Nm/rad	35113
Wheel Base, m	5.4		

[1] Front axle weight, [2] Center of gravity

All the tests were carried out using IPG/TruckMaker® Software-in-Loop (SiL) test bench along with MATLAB® software. Vehicle parameters used for the test runs were given in the Table 1. A total of 48 test runs were carried out to collect training data. For training the ANN model, two hidden layers were considered. The number of neurons in each layer was in the range of 1 neurons to 20 neurons and the number of epochs were varied from 10 to 200 with an increment of 10. By doing the simulations, the best choice for number of neurons were found as 7 (hidden layer 1) and 11 (hidden layer 2) and the number of iteration was fixed as 150. The prediction of side slip angle was carried out by collecting test data with both straight line and steady state circle maneuvering with random torque reductions. Some of the major results are given in Fig. 5. Here, the fault is introduced in the front right brake chamber. Figures 5(a) and 5(b) correspond to straight line maneuver with

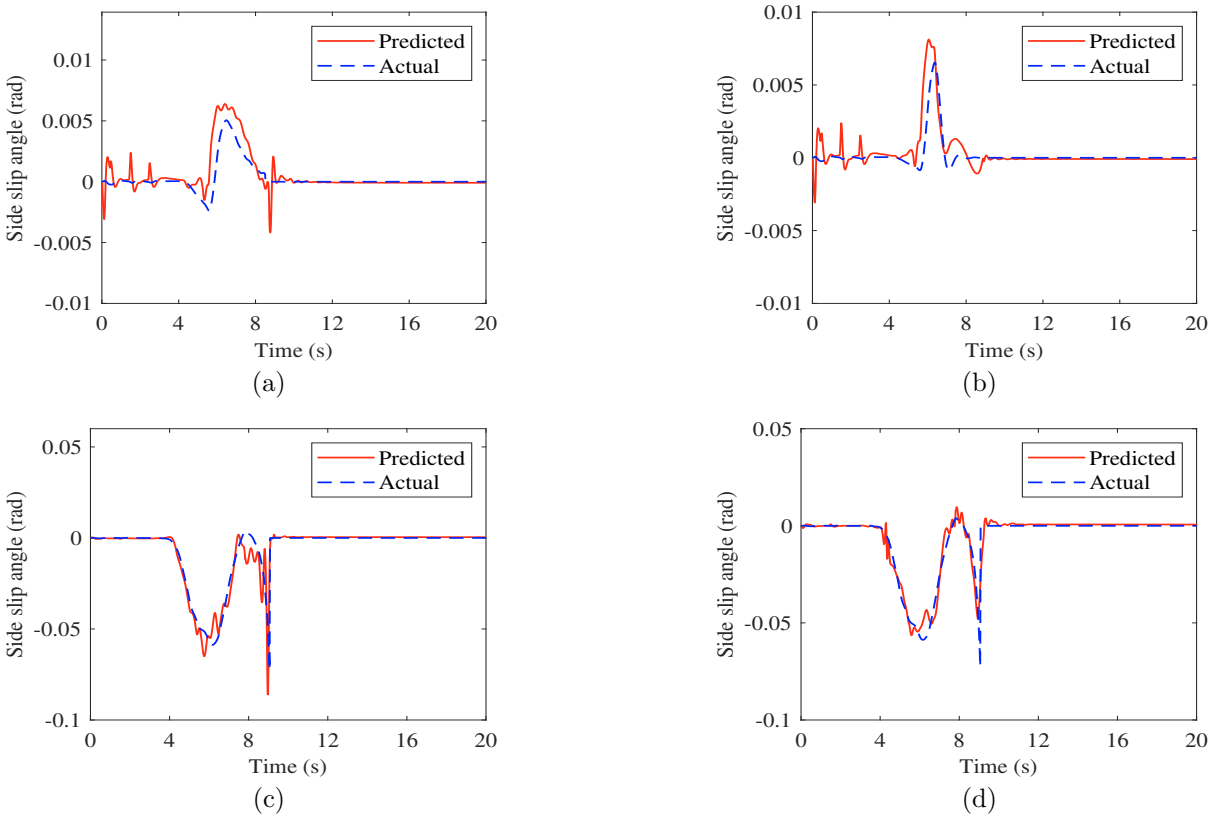

Fig. 5. Side slip angle estimation of a laden vehicle under full brake application with fault on front right brake: (a) Straight line maneuver with fault (15 % torque reduction), (b) Straight line maneuver with fault (25 % torque reduction), (c) Steady state circle maneuver with fault (15 % torque reduction), (d) Steady state circle maneuver with fault (25 % torque reduction)

brake torque reduction of 15 % and 25 % (equivalent to excessive stroke length) respectively. Similarly Fig. 5(c) and 5(d) correspond to steady state circle (radius 100 m) maneuver with brake torque reduction of 15 % and 25 % respectively. From these observations it is clear that, ANN based prediction scheme gave good accuracy in predicting side slip angle.

4. SLIDING MODE CONTROLLER DESIGN

Sliding Mode Controller (SMC) design approach is recognized as an efficient robust control strategy for various control engineering problems. The major advantage of SMC is its low sensitivity to external disturbances and parameter variations. Practically, SMC is characterized by high frequency control signal switching in the sliding mode that would result in the phenomenon of chattering (Hung et al. (1993)). SMC design is based on the selection of a suitable sliding surface that would restrict the system dynamics on to it, thus ensuring desired behaviour during sliding mode motion. This is achieved through the design of a discontinuous control equation that would maintain the system trajectory to the sliding surface (Wang et al. (2004)). In order to design the yaw angle correction controller for the air brake system using SMC, the control objective has been formulated as an output regulation problem with yaw angle, ψ as the output variable. Here, the error in output variable is

$$e(t) = y_a(t) - y_d(t) = \psi(t) - \psi_d(t), \tag{8}$$

where, $y_a(t)$ and $y_d(t)$ are actual and desired output respectively. $\psi_d(t)$, desired yaw angle is '0' for straight line maneuver. For the design of SMC, the sliding surface was defined as,

$$s(t) = \lambda e(t) + \dot{e}(t), \tag{9}$$

where, λ is the slope of sliding surface and $\lambda > 0$. Then,

$$\dot{s}(t) = \lambda \dot{e}(t) + \ddot{e}(t) \tag{10}$$

Now,

$$\dot{s}(t) = \lambda \dot{\psi}(t) + \ddot{\psi}(t) \tag{11}$$

The reaching law (Hung et al. (1993)) was chosen as

$$\dot{s}(t) = -K sign(s(t)) = \lambda \dot{\psi}(t) + \ddot{\psi}(t), \tag{12}$$

where, K is a positive constant. Using (12) and (2), the steering control signal δ(t) can now be obtained as,

$$\delta(t) = \frac{-K sign(s(t)) I_z}{2C_{\alpha f} l_f} - \left[\frac{\lambda I_z}{2C_{\alpha f} l_f} - \frac{C_{\alpha f} l_f^2 + C_{\alpha r} l_r^2}{C_{\alpha f} l_f V_x(t)}\right] \dot{\psi}(t) + \left[\frac{C_{\alpha f} l_f + C_{\alpha r} l_r}{C_{\alpha f} l_f}\right] \beta(t). \tag{13}$$

As already discussed, SMC is characterized by high frequency control signal switching, viz., chattering due to the presence of sign term in the control equation. During the practical realization of steering angle command for yaw angle correction, these high frequency control switching is not admissible. Hence, a boundary layer method was used to mitigate chattering which uses a saturation function

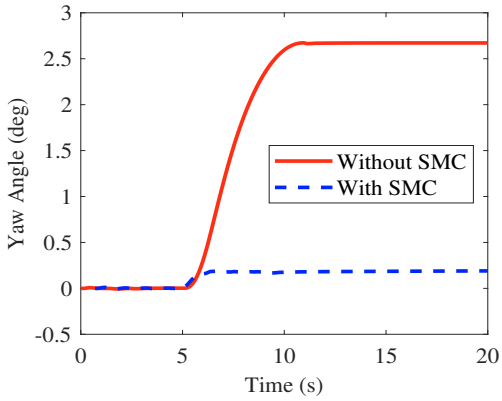

(a)

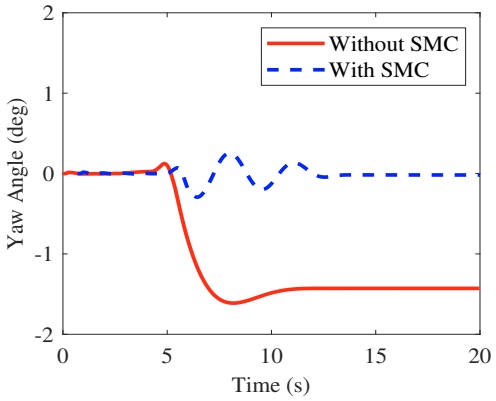

(b)

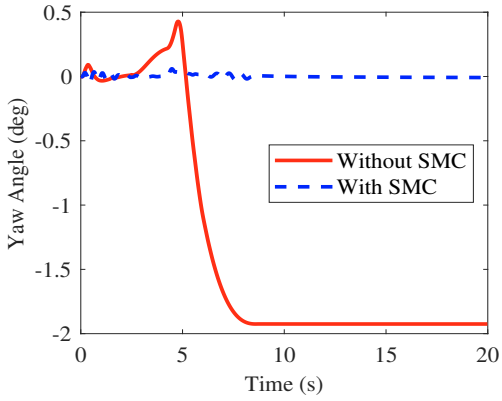

(c)

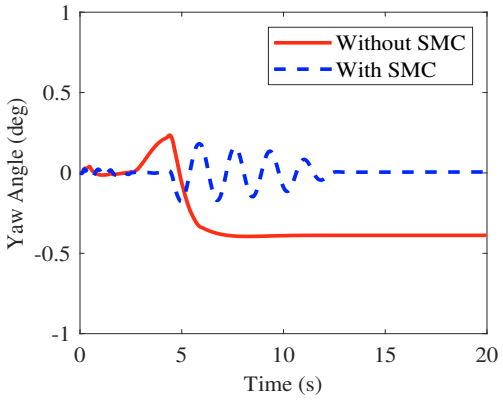

(d)

(e)

(f)

Fig. 6. Yaw angle correction using SMC with 30 % brake torque reduction (from full load torque) on front right brake under full brake application: (a) Fully laden vehicle with $\mu_{max} = 0.8$, (b) Fully laden vehicle with $\mu_{max} = 0.35$, (c) Fully unladen vehicle with $\mu_{max} = 0.8$, (d) Fully unladen vehicle with $\mu_{max} = 0.35$, (e) Vehicle (Fully laden, $\mu_{max} = 0.8$) Orientation without SMC controller, (f) Vehicle (Fully laden, $\mu_{max} = 0.8$) Orientation with SMC controller.

instead of the sign function in the control equation for smooth control action (Slotine (1984)).

5. RESULTS

In order to investigate the performance of the designed yaw angle controller, a fault was introduced in the front right brake chamber with 30 % brake torque reduction (from full load torque). This fault would ultimately cause a yaw angle deviation from straight line. This study has been conducted for both fully laden and fully unladen vehicle with tire road friction values of $\mu_{max} = 0.8$ and $\mu_{max} = 0.35$. The results are shown in Fig. 6. Figures 6(a) and 6(b) correspond to fully laden vehicle with maximum tire road friction coefficient of 0.8 (dry road) and 0.35 (snowy road) respectively. Figures 6(c) and 6(d) correspond to fully unladen vehicle. The steady state yaw angle values with and without controller are given in Table 2. It can

Table 2. Performance evaluation of SMC controller with 30 % brake torque reduction (from full load torque) on front right brake under full brake application

Vehicle type and tire road interface friction coefficient	**Yaw angle (deg) (Steady state)**		**Decrease in yaw angle (%)**
	Without SMC	**With SMC**	
Fully laden, $\mu_{max} = 0.8$	2.69	0.1797	93.4
Fully laden, $\mu_{max} = 0.35$	-1.612	0.0047	99.8
Fully unladen, $\mu_{max} = 0.8$	-1.925	0.0036	99.8
Fully unladen, $\mu_{max} = 0.35$	-0.3903	0.004	98.9

be observed that the controller was able to provide a percentage correction of steady state yaw angle of 93.4 % and 99.8 % respectively for fully laden and fully unladen vehicle with high friction tire road surface and the same corresponding to low friction tire road surface was 99.8 % and 98.9 % respectively. The controller was always able to regulate the yaw angle within a value less than $\pm$ 0.2^o and kept the vehicle in straight line even in the presence of a faulty brake. Also, the vehicle orientation without and with the controller is given in Fig. 6(e) and Fig. 6(f) respectively. Here, a truck with a length of 8.1 m and a track width of 2.1 m on a road with a lane width of 3.5 m was considered. A 30 % torque reduction on the front right brake chamber lead to a yaw angle deviation of 2.69^o from the straight line and caused the vehicle's departure from the original lane (Fig. 6(e)). The proposed controller was able to regulate the yaw angle to the desired value and the vehicle was kept within the lane as shown in Fig. 6(f).

6. CONCLUSION

This study developed a control algorithm to regulate the yaw angle in the presence of faulty brake in HCRVs. An ANN based estimation scheme was used to estimate side slip angle from the knowledge of steering angle, yaw rate, roll rate and vehicle longitudinal speed. Further, a controller based on SMC technique was developed to correct the vehicle yaw angle deviation due to the faults in vehicle brake system. Here, the SMC controller provided a steering angle to regulate the steady state yaw angle within the tolerance $\pm$ 0.2^o. The results showed that the controller effectively ensured vehicle directional stability by maintaining the yaw angle to the desired value.

REFERENCES

Abe, M. (2015). *Vehicle handling dynamics: theory and application*. Butterworth-Heinemann.

Chu, L., Shi, Y., Zhang, Y., Liu, H., and Xu, M. (2010). Vehicle lateral and longitudinal velocity estimation based on adaptive kalman filter. In *2010 3rd International Conference on Advanced Computer Theory and Engineering (ICACTE)*, volume 3, V3–325. IEEE.

Dhar, S. (2010). *Development of diagnostic algorithms for air brakes in trucks*. Texas A&M University.

Dunn, A.L., Guenther, D.A., and Radlinski, R. (2012). Application of air brake performance relationships in accident reconstruction and their correlation to real vehicle performance. *SAE International Journal of Commercial Vehicles*, 5(2012-01-0609), 251–270.

Gao, Y., Feng, Y., and Xiong, L. (2013). Vehicle longitudinal velocity estimation with adaptive kalman filter. In *Proceedings of the FISITA 2012 World Automotive Congress*, 415–423. Springer.

Hebden, R.G., Edwards, C., and Spurgeon, S.K. (2003). An application of sliding mode control to vehicle steering in a split-mu maneuver. In *Proceedings of the 2003 American Control Conference, 2003.*, volume 5, 4359–4364. IEEE.

Hung, J.Y., Gao, W., and Hung, J.C. (1993). Variable structure control: A survey. *IEEE transactions on industrial electronics*, 40(1), 2–22.

Kandt, L., Reinhall, P., and Scheibe, R. (2001). Determination of air brake adjustment from air pressure data. *Proceedings of the Institution of Mechanical Engineers, Part D: Journal of Automobile Engineering*, 215(1), 21–29.

Kazemi, R. and Janbakhsh, A. (2010). Nonlinear adaptive sliding mode control for vehicle handling improvement via steer-by-wire. *International journal of automotive technology*, 11(3), 345–354.

Radlinski, R.W., Williams, S.F., and Machey, J.M. (1982). The importance of maintaining air brake adjustment. *SAE Transactions*, 4074–4085.

Ramarathnam, S., Dhar, S., Darbha, S., and Rajagopal, K. (2011). Development of a model for an air brake system with leaks and a scheme for the estimation of the steady-state pushrod stroke. *Vehicle System Dynamics*, 49(8), 1267–1282.

Raveendran, R., Suresh, A., Rajaram, V., and Subramanian, S.C. (2018). Artificial neural network approach for air brake pushrod stroke prediction in heavy commercial road vehicles. *Proceedings of the Institution of Mechanical Engineers, Part D: Journal of Automobile Engineering*. URL `https://doi.org/10.1177/0954407018794594`.

Slotine, J.J.E. (1984). Sliding controller design for nonlinear systems. *International Journal of control*, 40(2), 421–434.

Song, C.K., Uchanski, M., and Hedrick, J.K. (2002). Vehicle speed estimation using accelerometer and wheel speed measurements. Technical report, SAE Technical Paper.

Subramanian, S.C., Darbha, S., and Rajagopal, K. (2006). A diagnostic system for air brakes in commercial vehicles. *IEEE Transactions on Intelligent Transportation systems*, 7(3), 360–376.

Wang, W., Yi, J., Zhao, D., and Liu, D. (2004). Design of a stable sliding-mode controller for a class of second-order underactuated systems. *IEE Proceedings-Control Theory and Applications*, 151(6), 683–690.

Zhou, H. and Liu, Z. (2010). Vehicle yaw stability-control system design based on sliding mode and backstepping control approach. *IEEE Transactions on Vehicular Technology*, 59(7), 3674–3678.